

MULTI-DIMENSIONAL SPACE-TIME-FREQUENCY COMPONENT ANALYSIS OF EVENT RELATED EEG DATA USING CLOSED-FORM PARAFAC

Martin Weis, Florian Römer, Martin Haardt

Ilmenau University of Technology
Communications Research Laboratory
D-98684 Ilmenau, Germany

Dunja Jannek, Peter Husar

Ilmenau University of Technology
Biosignal Processing Group
D-98684 Ilmenau, Germany

Abstract — The efficient analysis of electroencephalographic (EEG) data is a long standing problem in neuroscience, which has regained new interest due to the possibilities of multidimensional signal processing. We analyze event related multi-channel EEG recordings on the basis of the time-varying spectrum for each channel. It is a common approach to use wavelet transformations for the time-frequency analysis (TFA) of the data. To identify the signal components we decompose the data into time-frequency-space atoms using Parallel Factor (PARAFAC) analysis. In this paper we show that a TFA based on the Wigner-Ville distribution together with the recently developed closed-form PARAFAC algorithm enhance the separability of the signal components. This renders it an attractive approach for processing EEG data. Additionally, we introduce the new concept of component amplitudes, which resolve the scaling ambiguity in the PARAFAC model and can be used to judge the relevance of the individual components.

Index Terms— Tensor, Multi-dimensional signal processing, PARAFAC, Event Related EEG, Wigner-Ville Distribution

1. INTRODUCTION

In this contribution we focus on analyzing measured electroencephalographic (EEG) data to find the components of specific activity on the scalp. This analysis can also be used to detect and localize epileptic seizure onset zones on the scalp as well as projections of cognitive processing like speech or auditory handling. Unfortunately, different sources in the brain can produce the same EEG pattern on the scalp, which renders them in general non-separable. Source localization algorithms, such as LORETA [11] or dipole fitting methods can resolve this ambiguity by imposing additional assumptions. For further improvements of these methods, preprocessing in form of subspace decompositions, e.g., Principle Component Analysis (PCA), Independent Component Analysis (ICA), Singular Value Decomposition (SVD), or beamforming algorithms [6] have been applied. However, these methods cannot exploit the multi-dimensional nature of the EEG data. Moreover, to obtain matrix decompositions like PCA or ICA, physically irrelevant assumptions like orthogonality or independence have to be imposed. Therefore, tensor decompositions are a more promising approach to handle EEG signals. Especially the well known Parallel Factor (PARAFAC) analysis is a powerful tool for analyzing EEG data, because it is essentially unique under mild conditions [1] without any artificial constraints, such as orthogonality. In the last years PARAFAC was applied to EEG signals, e.g., for estimating sources of cognitive processing [9], for the analysis of event related potentials (ERP) [10], and for epileptic seizure localization [16].

In order to resolve the temporal evolution as well as the frequency content of the EEG recordings, a time-frequency analysis (TFA) is applied for each channel. Therefore, the data is analyzed

over three dimensions, i.e., time, frequency, and space (channels). Different TFA algorithms have been studied for the analysis of EEG signals [5]. The most common time-frequency decomposition is the continuous wavelet transformation (CWT) [14]. However, we have shown in [7] that wavelet analysis may not provide adequate time and frequency resolution for EEG data.

In this contribution we use a TFA method based on the Wigner-Ville distribution. Thereby, we suppress the effect of cross terms by using the reduced interference distribution [5]. This method shows a significantly improved time-frequency resolution and therefore also improves the PARAFAC analysis. We compare the results to the standard wavelet based techniques. For the computation of the PARAFAC decomposition the most common methods to date are based on iterative alternating least squares (ALS) algorithms. However, these algorithms may require many iterations and are not guaranteed to converge to the global minimum. The recently developed closed-form PARAFAC algorithm [12, 13] outperforms the iterative approaches. Therefore, we use it to decompose the time-frequency distributions into time-frequency-space atoms and to identify the different signal components of the EEG data.

This paper is organized as follows: In Section 2 we clarify the notation and define the operators and symbols that are used. In Section 3 we discuss the signal processing steps to process EEG signals. Then, Section 3.1 briefly presents the methods for the time-frequency analysis of the EEG data and Section 3.2 describes the closed-form PARAFAC decomposition. Here we also show how to resolve the scaling ambiguities in the PARAFAC model. In Section 4 we present the results of the event related EEG analysis based on measurements, before drawing the conclusions in Section 5.

2. NOTATION

To facilitate the distinction between scalars, vectors, matrices, and higher-order tensors, we use the following notation: scalars are denoted by lower-case italic letters (a, b, \dots), vectors by boldface lower-case italic letters ($\mathbf{a}, \mathbf{b}, \dots$), matrices by boldface upper-case letters ($\mathbf{A}, \mathbf{B}, \dots$), and tensors are denoted as upper-case, boldface, calligraphic letters ($\mathcal{A}, \mathcal{B}, \dots$). This notation is consistently used for lower-order parts of a given structure. For example $\mathcal{A} \in \mathbb{C}^{I_1 \times I_2 \times \dots \times I_N}$ represents an N -dimensional tensor of size I_n along mode n . Its elements are referenced by a_{i_1, i_2, \dots, i_N} for $i_n = 1, 2, \dots, I_n$ and $n = 1, 2, \dots, N$. Furthermore, the i -th column vector of a matrix \mathbf{A} is denoted as \mathbf{a}_i . For matrices we use the superscripts $\text{T}, \text{H}, ^{-1}, +$ for transposition, Hermitian transposition, matrix inverse, and Moore-Penrose pseudo-inverse, respectively. The Kronecker product and the Khatri-Rao product (column-wise Kronecker product) of two matrices \mathbf{A} and \mathbf{B} are expressed by $\mathbf{A} \otimes \mathbf{B}$ and $\mathbf{A} \diamond \mathbf{B}$, respectively.

The tensor operations we use are consistent with [8]. The higher-order norm of a tensor \mathcal{A} , symbolized by $\|\mathcal{A}\|_{\text{H}}$, is de-

defined as the square root of the sum of the squared magnitude of all elements in \mathcal{A} . The n -mode vectors of a tensor \mathcal{A} are obtained by varying the n -th index i_n of the tensor elements a_{i_1, i_2, \dots, i_N} within its range $(1, 2, \dots, I_n)$ while keeping all the other indices fixed. The matrix unfolding of the tensor \mathcal{A} , denoted by $[\mathcal{A}]_{(n)} \in \mathbb{C}^{I_n \times I_1 \times \dots \times I_{n-1} \times I_{n+1} \times \dots \times I_N}$ contains all the n -mode vectors of the tensor \mathcal{A} . The n -mode product of a tensor $\mathcal{A} \in \mathbb{C}^{I_1 \times \dots \times I_N}$ and a matrix $\mathbf{U} \in \mathbb{C}^{J_n \times I_n}$ is denoted as $(\mathcal{A} \times_n \mathbf{U}) \in \mathbb{C}^{I_1 \times \dots \times J_n \times \dots \times I_N}$. It is obtained by multiplying all n -mode vectors of \mathcal{A} from the left hand side by the matrix \mathbf{U} . The outer product of an N -dimensional tensor \mathcal{A} and a K -dimensional tensor \mathcal{B} , denoted by $(\mathcal{A} \circ \mathcal{B})$, is a $(N + K)$ -dimensional tensor whose elements are given by $(\mathcal{A} \circ \mathcal{B})_{i_1, \dots, i_N, j_1, \dots, j_K} = a_{i_1, \dots, i_N} \cdot b_{j_1, \dots, j_K}$. An N -dimensional tensor $\mathcal{A} \in \mathbb{C}^{I_1 \times \dots \times I_N}$ is of rank one if and only if it can be written as the outer product between N non-zero vectors $\mathbf{c}^{(n)} \in \mathbb{C}^{I_n}$, such that $\mathcal{A} = \mathbf{c}^{(1)} \circ \dots \circ \mathbf{c}^{(N)}$. The three-dimensional identity tensor $\mathcal{I}_{3,d}$ is defined as

$$\mathcal{I}_{3,d} = \sum_{n=1}^d \mathbf{e}_{n,d} \circ \mathbf{e}_{n,d} \circ \mathbf{e}_{n,d} \in \mathbb{R}^{d \times d \times d}, \quad (1)$$

where $\mathbf{e}_{n,d}$ represents the n -th column of a $d \times d$ identity matrix (also termed the n -th pinning vector of size d).

3. SIGNAL PROCESSING STEPS

The processing of EEG data is a very challenging task due to the complex nature of these signals, e.g., they are non-stationary and suffer from very low signal to noise ratios. Moreover, they are affected by correlated noise with unknown distribution and artifacts originating from eye blinks, eye movements, and muscle movements as well as from diverse technical and biological distortions. Therefore, a

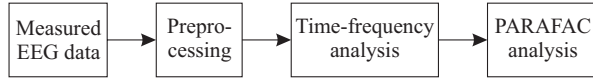


Fig. 1. Signal processing steps for the identification of signal components in event-related EEG data.

suitable preprocessing has to be applied in the form of filters, reference EEG channels, and averaging over numerous trials. Furthermore, the EEG data has to be divided into smaller stationary time windows. Afterwards, the time-frequency analysis is applied to each channel individually, in order to resolve the temporal evolution as well as the frequency content of the EEG data. The components of the resulting three-way signal, which changes in frequency, space (channels), and time, are extracted via parallel factor (PARAFAC) analysis (see Figure 1).

3.1. Time-Frequency Analysis

There exist a large number of methods that can be applied to decompose EEG signals into their time-frequency content [5]. An approach that is very often used is the continuous wavelet transformation (CWT). The continuous wavelet transform $C(a, \tau)$ at scale a of a signal $x(t)$ is defined as

$$C(a, \tau) = \int_{-\infty}^{\infty} x(t) \varphi(a, t, \tau) dt, \quad (2)$$

where φ is the chosen wavelet. Common choices include the class of biorthogonal wavelets, Debauchy wavelets, and the Morlet wavelets [14]. The connection between the scale a and the frequency f is given by

$$f \approx \frac{f_c}{a \cdot \Delta t}, \quad (3)$$

where f_c is the center frequency of the wavelet and Δt is the sampling interval for $x(t)$. The disadvantage of CWT-based time-frequency preprocessing is the limited resolution, especially in the low-frequency region, which is very important in EEG signal analysis.

A more powerful approach to time-frequency analysis is given by the family of Wigner-Ville distribution functions, based on the seminal work of Wigner [17] in 1932 and Ville [15] in 1948. The distribution is based on the temporal correlation function (TCF) $q_x(t, \tau)$ of the signal $x(t)$ which is defined as [5]

$$q_x(t, \tau) = x\left(t + \frac{\tau}{2}\right) x^*\left(t - \frac{\tau}{2}\right). \quad (4)$$

The Wigner-Ville distribution (WVD) $W_x(t, f)$ of $x(t)$ is defined as the Fourier transform of the TCF with respect to the lag variable τ

$$W_x(t, f) = \int_{-\infty}^{\infty} q_x(t, \tau) e^{-j2\pi f \tau} d\tau. \quad (5)$$

Therefore, the WVD is a quadratic, real-valued time-frequency distribution (TFD). The ambiguity function $A_x(\theta, \tau)$ is symmetric in τ and is defined as the inverse Fourier transform of the TCF with respect to the time t [5]

$$A_x(\theta, \tau) = \int_{-\infty}^{\infty} q_x(t, \tau) e^{j2\pi \theta t} dt. \quad (6)$$

Thus, the ambiguity function and the Wigner-Ville distribution are related by the two-dimensional Fourier transform. The main drawback of the time-frequency analysis based on the TCF is that it produces cross terms in $W_x(t, f)$ as well as in $A_x(\theta, \tau)$. On the other hand, its advantage is that time and frequency resolution can be adjusted separately. In 1966 Cohen introduced an overall class of TFDs based on the WVD which allow the use of kernel functions for reducing cross terms [4]. This group of TFDs $P_x(t, f)$ is defined as

$$P_x(t, f) = \int_{-\infty}^{\infty} \int_{-\infty}^{\infty} A_x(\theta, \tau) \Theta(\theta, \tau) e^{-j2\pi \theta t - j2\pi \tau f} d\theta d\tau, \quad (7)$$

where $\Theta(\theta, \tau)$ is the kernel function. A large number of TFDs have been proposed, each differing only in the choice of $\Theta(\theta, \tau)$. These kernel functions can be used to suppress the effect of the cross terms on the TFD. Choi and Williams [3] introduced the reduced interference distribution (RID), which is a TFD based on the exponential kernel function

$$K(\theta, \tau) = e^{-\frac{\theta^2 \tau^2}{\sigma}}, \quad (8)$$

where $\sigma > 0$ is a scaling factor which influences the cross term suppression.

3.2. Three-Way PARAFAC Analysis

After the time-frequency analysis the EEG data is represented by time-varying frequency distributions for every channel. This three-way data can be expressed in form of a tensor

$$\mathcal{X} \in \mathbb{R}^{N_F \times N_T \times N_C}, \quad (9)$$

where N_F and N_T are the number of samples in frequency and time, and N_C is the number channels, respectively. In order to separate the signal components in this tensor, we use a multi-dimensional extension of the singular value decomposition that is known as the PARAFAC decomposition [1]. Thereby, we decompose a tensor into

a minimal sum of rank one components. In the absence of noise, the PARAFAC model for the tensor (9) can be represented as

$$\mathcal{X} = \sum_{n=1}^d \mathbf{a}_n \circ \mathbf{b}_n \circ \mathbf{c}_n, \quad (10)$$

where the vectors $\mathbf{a}_n \in \mathbb{R}^{N_F}$, $\mathbf{b}_n \in \mathbb{R}^{N_T}$, and $\mathbf{c}_n \in \mathbb{R}^{N_C}$, represent the frequency, time, and space (channel) signatures of the n -th PARAFAC component. Moreover, d represents the number of signal components. In practice the PARAFAC model does not fit the data exactly for a number of reasons:

- The measured EEG data is affected by correlated noise with an unknown distribution. The signal to noise ratio is very low.
- The signal components are not necessarily rank one. The number of signal components is unknown.
- The superposition of the components is not linear.

Therefore, we require a robust algorithm for the computation of an approximate fit of the PARAFAC model to the data tensor \mathcal{X} . Among the many existing PARAFAC methods we propose to use the recently developed closed-form PARAFAC algorithm [12, 13]. This algorithm is based on the higher order singular value decomposition (HOSVD) of \mathcal{X} which is defined as [8]

$$\mathcal{X} = \mathcal{S} \times_1 \mathbf{U}_1 \times_2 \mathbf{U}_2 \times_3 \mathbf{U}_3, \quad (11)$$

where $\mathcal{S} \in \mathbb{R}^{N_F \times N_T \times N_C}$ is the full core tensor of same size as \mathcal{X} . The unitary matrices $\mathbf{U}_1 \in \mathbb{R}^{N_F \times N_F}$, $\mathbf{U}_2 \in \mathbb{R}^{N_T \times N_T}$ and $\mathbf{U}_3 \in \mathbb{R}^{N_C \times N_C}$ provide an orthonormal basis for the 1-, 2-, and 3-mode vector spaces of \mathcal{X} , respectively. Thus, the HOSVD can easily be obtained from the matrix singular value decomposition of the n -mode matrix unfoldings of \mathcal{X} [8]. In the non-degenerate case ($d \leq \min\{N_F, N_T, N_C\}$) the HOSVD of the tensor \mathcal{X} can be truncated to

$$\mathcal{X} = \mathcal{S}^{[d]} \times_1 \mathbf{U}_1^{[d]} \times_2 \mathbf{U}_2^{[d]} \times_3 \mathbf{U}_3^{[d]}, \quad (12)$$

where $\mathcal{S}^{[d]} \in \mathbb{R}^{d \times d \times d}$ and where $\mathbf{U}_1^{[d]}$, $\mathbf{U}_2^{[d]}$ and $\mathbf{U}_3^{[d]}$ are of size $(N_F \times d)$, $(N_T \times d)$, and $(N_C \times d)$, respectively. By defining the set of matrices $\mathbf{A} = [\mathbf{a}_1, \dots, \mathbf{a}_d] \in \mathbb{R}^{N_F \times d}$, $\mathbf{B} = [\mathbf{b}_1, \dots, \mathbf{b}_d] \in \mathbb{R}^{N_T \times d}$, and $\mathbf{C} = [\mathbf{c}_1, \dots, \mathbf{c}_d] \in \mathbb{R}^{N_C \times d}$ we can rewrite the PARAFAC model (10) in terms of the identity tensor $\mathcal{I}_{3,d}$

$$\mathcal{X} = \mathcal{I}_{3,d} \times_1 \mathbf{A} \times_2 \mathbf{B} \times_3 \mathbf{C}. \quad (13)$$

Comparing the equations (12) and (13) indicates that there is a link between the PARAFAC model and the HOSVD. To exploit this connection we introduce the transformation matrices $\mathbf{T}_1 \in \mathbb{R}^{d \times d}$, $\mathbf{T}_2 \in \mathbb{R}^{d \times d}$, and $\mathbf{T}_3 \in \mathbb{R}^{d \times d}$ such that

$$\mathbf{A} = \mathbf{U}_1^{[d]} \cdot \mathbf{T}_1, \mathbf{B} = \mathbf{U}_2^{[d]} \cdot \mathbf{T}_2, \mathbf{C} = \mathbf{U}_3^{[d]} \cdot \mathbf{T}_3. \quad (14)$$

Inserting these equations into (13) and comparing it with (12) yields

$$\mathcal{S}^{[d]} \times_1 \mathbf{T}_1^{-1} \times_2 \mathbf{T}_2^{-1} \times_3 \mathbf{T}_3^{-1} = \mathcal{I}_{3,d}. \quad (15)$$

Therefore, the closed-form PARAFAC algorithm estimates the transformation matrices that diagonalize the truncated core tensor $\mathcal{S}^{[d]}$ to the identity tensor $\mathcal{I}_{3,d}$. In [12, 13] it is shown that this can be accomplished very efficiently by means of joint matrix diagonalizations, also in the degenerate case. The resulting closed-form algorithm outperforms iterative approaches especially in critical scenarios, since it does not require alternating least squares iterations. Moreover, it provides the opportunity to obtain a tradeoff between accuracy and computational time.

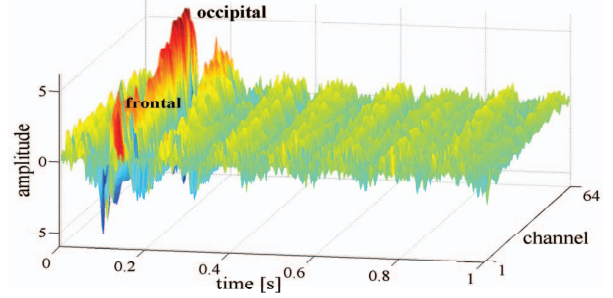


Fig. 2. Time evolution of all 64 EEG channels. The data is averaged over 1600 trials of a 20 ms light flash to the right eye of a 23 years old healthy woman. We can see that the occipital channels show the response earlier than the frontal ones.

3.2.1. Scaling ambiguity in PARAFAC

The PARAFAC model (10) is unique under mild conditions up to a scaling ambiguity for the component vectors \mathbf{a}_n , \mathbf{b}_n , and \mathbf{c}_n and a permutation of the components $\mathbf{a}_n \circ \mathbf{b}_n \circ \mathbf{c}_n$. Due to the non-orthogonality of the PARAFAC decomposition, the higher order norms of the component tensors $\mathbf{a}_n \circ \mathbf{b}_n \circ \mathbf{c}_n$ do not add up to the higher-order norm of \mathcal{X} . Bro [1] suggested to judge the influence of each of the components based on $\|\mathcal{X} - \mathbf{a}_n \circ \mathbf{b}_n \circ \mathbf{c}_n\|_H$. Because of the unknown dependency between the components, we suggest to fit all components jointly to the original data tensor \mathcal{X} in a least squares sense. Therefore, we normalize all component vectors to unit Frobenius norm, such that

$$\mathbf{a}'_n = \frac{\mathbf{a}_n}{\|\mathbf{a}_n\|_F}, \mathbf{b}'_n = \frac{\mathbf{b}_n}{\|\mathbf{b}_n\|_F}, \mathbf{c}'_n = \frac{\mathbf{c}_n}{\|\mathbf{c}_n\|_F} \quad \forall n = 1, \dots, d. \quad (16)$$

Note that this normalization leads to $\|\mathbf{a}'_n \circ \mathbf{b}'_n \circ \mathbf{c}'_n\|_H = 1$ for all $n = 1, \dots, d$. Next we introduce the PARAFAC component amplitudes γ_n for $n = 1, \dots, d$ by

$$\mathcal{X} \approx \sum_{n=1}^d \gamma_n \cdot \mathbf{a}'_n \circ \mathbf{b}'_n \circ \mathbf{c}'_n. \quad (17)$$

To determine all amplitudes jointly we rewrite this equation according to

$$\begin{aligned} \text{vec}(\mathcal{X}) &= [\text{vec}(\mathbf{a}'_1 \circ \mathbf{b}'_1 \circ \mathbf{c}'_1), \dots, \text{vec}(\mathbf{a}'_d \circ \mathbf{b}'_d \circ \mathbf{c}'_d)] \cdot \boldsymbol{\gamma} \\ &= (\mathbf{C}' \diamond \mathbf{B}' \diamond \mathbf{A}') \boldsymbol{\gamma}, \end{aligned} \quad (18)$$

where the matrices $\mathbf{A}' = [\mathbf{a}'_1, \dots, \mathbf{a}'_d]$, $\mathbf{B}' = [\mathbf{b}'_1, \dots, \mathbf{b}'_d]$, and $\mathbf{C}' = [\mathbf{c}'_1, \dots, \mathbf{c}'_d]$ contain the normalized component vectors. The vector $\boldsymbol{\gamma} = [\gamma_1, \dots, \gamma_d]^T$ contains all component amplitudes. The least squares solution for the set of linear equations (18) is given by

$$\boldsymbol{\gamma} = (\mathbf{C}' \diamond \mathbf{B}' \diamond \mathbf{A}')^+ \text{vec}(\mathcal{X}). \quad (19)$$

In practical applications the PARAFAC model often does not exactly fit the data, and no apriori knowledge can be used to resolve the scaling and permutation ambiguity. In these cases we suggest to judge the influence of the components based on the magnitudes of the component amplitudes γ_n . Please notice that for the real valued case the normalized model (17) still has a sign ambiguity, e.g., two of the three component vectors can be multiplied by minus one without changing the rank one component.

4. EXPERIMENTAL RESULTS

The EEG signal is recorded from a 23 year old woman, healthy and right-handed. The position of the 64 EEG electrodes is based on the international 10-10-system [2] with earlobe references $[(A1 + A2)/2]$. The sampling frequency is chosen to 1000 Hz. For the pre-processing of the raw signal, several filters are applied: a 7 Hz high-pass, a 135 Hz low-pass and a band-stop filter between 45 and 55 Hz. For the investigation of effects in the field of event related potentials, we record EEG data triggered as a function of a visual stimulus. The subject sits in front of a hemispherical perimeter. The stimulus is a 20 ms central light flash from a white LED to the right eye. The triggered EEG responses to this stimulus are averaged over 1600 trials for all channels (see Figure 2). For the signal component analysis

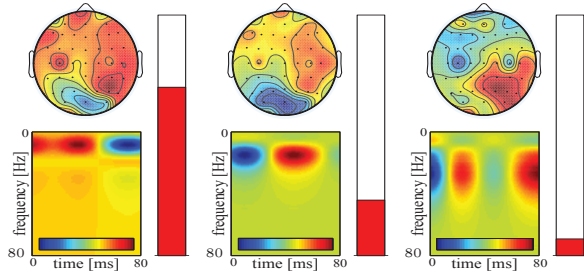


Fig. 3. Signal components for the TFA based on CWT with Morlet wavelets. The components are represented as topographic plots of the space signatures (top), together with the time-frequency signatures (bottom). The bars left to each component represent the relative magnitude of the PARAFAC amplitudes. The analysis window reaches from 101 to 180 ms.

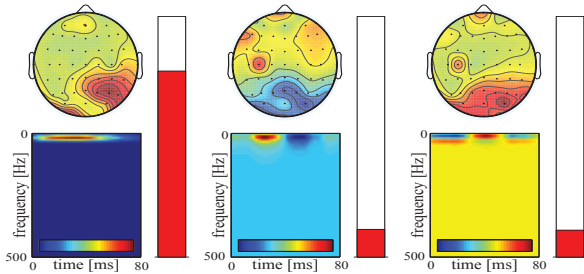


Fig. 4. Signal components for the TFA based on the reduced interference distribution. The analysis window reaches from 101 to 180 ms. Due to the increased time-frequency resolution the desired components are clearly revealed.

we divide the recorded EEG data into windows of length 80 ms to assure stationarity. In each window we apply two different methods for the time-frequency analysis: the CWT based on Morlet wavelets and the reduced interference distribution (RID, see Section 3.1). Afterwards, we use the closed-form PARAFAC algorithm (Section 3.2) to identify the signal components. The PARAFAC model is normalized according to equation (17). The number of components is set to three, and they are ordered according to the magnitude of the PARAFAC amplitudes defined in Section 3.2.1. Figure 3 shows the results for the time window between 100 ms and 180 ms based on the CWT with Morlet wavelets. The components are represented as a topographic plot of the space signatures, together with the associated time-frequency signature. The bar on the left of each component represents the relative magnitude of its PARAFAC amplitude. From previous studies based on potential mapping, a strong component in the lower right hemisphere (visual cortex) is expected. Because of the insufficient time resolution for low frequencies and the small frequency resolution for high frequencies, the desired component cannot be identified with the CWT. However, the desired component is

clearly represented in the results based on the RID time-frequency analysis (Figure 4). The comparison of the time-frequency signatures of both results clearly reveals the improved time and frequency resolution of the RID. This leads to an increased spatial resolution of the signal components.

5. CONCLUSIONS

In this contribution we have shown that an appropriate time-frequency analysis (TFA) scheme is an important factor for the identification of signal components in EEG data. We have shown that Wigner-Ville distribution based TFA methods provide an increased time-frequency resolution, which leads to an increased spatial resolution of the signal components. The effect of cross terms can be suppressed by using the reduced interference distribution (RID). This technique provides particularly instructive results in combination with the closed-form PARAFAC algorithm to identify the signal components in measured event related EEG data. In order to judge the influence of the different components we have introduced the novel component amplitudes, which resolve the scaling ambiguity in the PARAFAC model.

ACKNOWLEDGMENTS

The authors gratefully acknowledge the partial support of the internal excellence initiative at Ilmenau University of Technology.

REFERENCES

- [1] R. Bro, "PARAFAC. tutorial and applications", in *Chemometrics and Intelligent Laboratory Systems*, 38, pp. 149 – 171, 1997.
- [2] G.E. Chatrjian, E. Lettich, and P.L. Nelson, "Ten percent electrode system for topographic studies of spontaneous and evoked EEG activities.", in *American Journal of EEG Technology*, vol. 25, pp. 83–92, 1985.
- [3] H. Choi and W.J. Williams, "Improved time-frequency representation of multi-component signals using exponential kernels", in *IEEE Trans. Acoust., Speech, Signal Process.*, vol. 37, no. 6, pp. 862–871, 1989.
- [4] L. Cohen, "Time-frequency analysis: Theory and applications", Prentice Hall, Upper Saddle River, NJ, 1995.
- [5] C.M. Guerrero, A.M. Triguerosand, and J.I. Franco, "Time-frequency EEG analysis in epilepsy: What is more suitable?", in *Proceedings of the Fifth IEEE International Symposium on Signal Processing and Information Technology*, pp. 202 – 207, Athens, Greece, 2005.
- [6] P. Husar, S. Berkes, and M. Drozd, "An approach to adaptive beamforming in measurement of EEG", in *Proc. of the European Biomedical Engineering Congress (EMBECE)*, pp. 1438 – 1439, Vienna, Austria, 2002.
- [7] D. Jannek, F. Roemer, M. Weis, M. Haardt, and P. Husar, "Identification of signal components in multi-channel EEG signals via closed-form PARAFAC analysis and appropriate preprocessing", *European Biomedical Engineering Congress (EMBECE)*, Antwerp, Belgium, November, 2008, scheduled to appear.
- [8] L. De Lathauwer, B. de Moor, and J. Vandewalle, "A multilinear singular value decomposition", *SIAM J. Matrix Anal. Appl.*, vol. 21, no. 4, 2000.
- [9] F. Miwakeichi, E. Martinez-Montes, and P.A. Valdés-Sosa, "Decomposing EEG data into space-time-frequency components using parallel factor analysis", in *NeuroImage* 22(3), pp. 1035–1045, 2004.
- [10] M. Mørup, L.K. Hansen, and C.S. Hermann, "Parallel factor analysis as an exploratory tool for wavelet transformed event-related EEG", in *NeuroImage* 29(3), pp. 938–947, 2006.
- [11] R.D. Pascual-Marqui, C.M. Michel, and D. Lehmann, "Low resolution electromagnetic tomography: A new method for localizing electrical activity in the brain", in *Int J Psychophysiol* 18, pp. 49 – 65, 1994.
- [12] F. Roemer and M. Haardt, "A closed-form solution for multilinear PARAFAC decompositions", in *Proc. 5-th IEEE Sensor Array and Multichannel Signal Processing Workshop (SAM 2008)*, pp. 487 – 491, Darmstadt, Germany, July 2008.
- [13] F. Roemer and M. Haardt, "A closed-form solution for parallel factor (PARAFAC) analysis", in *Proc. IEEE Int. Conf. Acoust., Speech, and Signal Processing (ICASSP)*, pp. 2365–2368, Las Vegas, NV, April 2008.
- [14] C. Torrence and G. Compo, "A practical guide to wavelet analysis", in *Bull Amer Meteorol* 79(1), pp. 61–78, 1998.
- [15] J. Ville, "Théorie et applications de la notion de signal analytique", in *Câbles et transmissions*, vol. 2A, pp. 66–74, 1948.
- [16] M. De Vos, L. De Lathauwer, and B. Vanrumste, "Canonical decomposition of ictal scalp EEG and accurate source localisation: Principles and simulation study", in *Comput. Intell. Neurosci.*, 2007.
- [17] E.P. Wigner, "On the quantum correction for thermodynamic equilibrium", in *Phys. Rev.*, vol. 40, pp. 749–759, 1932.